

# The ATLAS jet trigger for Run 3 of the LHC

Maximilian Amerl<sup>1,\*</sup>, on behalf of the ATLAS Collaboration

<sup>1</sup>The University of Manchester

**Abstract.** The ATLAS jet trigger is instrumental in selecting events both for Standard Model measurements and Beyond the Standard Model physics searches. Non-standard triggering strategies, such as storing only a small fraction of trigger objects for each event, avoids bandwidth limitations and increases sensitivity to low-mass and low-momentum objects. These events are used by Trigger Level Analyses, which can reach regions of parameter space that would otherwise be inaccessible. To this end, the calibration of trigger-level jets is imperative both to ensure good trigger performance across the ATLAS physics programme and to provide well-measured jets for Trigger Level Analysis. This contribution presents an introduction to the ATLAS jet trigger for Run-3 of the LHC and discusses the performance of the trigger jet calibration. These studies will allow us to commission a Run-3 trigger jet calibration that provides excellent performance across a broad jet transverse momentum range starting from 25 GeV.

## 1 Introduction

Jets are an experimental signature of the hadronisation of quarks and gluons detected as collimated bursts of charged and neutral particles. Since many Standard Model and Beyond the Standard Model physics signatures involve jets, it is important to be able to both measure jets well and select events in which they feature. The ATLAS jet trigger plays an important role during data-taking. In preparation for Run 3, a number of improvements have been made to the ATLAS jet trigger, allowing it to perform well in more demanding LHC collision conditions. The following paper introduces these changes and presents measured (2022) and expected (2023) trigger-level jet performance results.

### 1.1 Configuration of the ATLAS jet trigger for Run 3

The ATLAS<sup>1</sup> trigger system shown in Figure 1 consists of a two-level hardware and software trigger system. The first stage, the Level-1 (L1) hardware trigger, makes low-latency (2.5  $\mu$ s)

---

© 2023 CERN for the benefit of the ATLAS Collaboration. Reproduction of this article or parts of it is allowed as specified in the CC-BY-4.0 license.

\*e-mail: maximilian.amerl@cern.ch

<sup>1</sup>The ATLAS experiment uses a right-handed coordinate system to describe the position of objects in the detector [1]. The pseudo-rapidity,  $\eta$ , is defined as  $-\ln(\tan(\theta/2))$  in terms of the polar coordinate,  $\theta$ , measured between the beam ( $z$ ) axis and vertical  $y$ -axis [1]. The azimuthal angle,  $\phi$ , is measured around the beam axis [1]. The angular distance between two objects in the detector is calculated as  $\Delta R = \sqrt{(\Delta\eta)^2 + (\Delta\phi)^2}$  in terms of the differences in their angular coordinates.

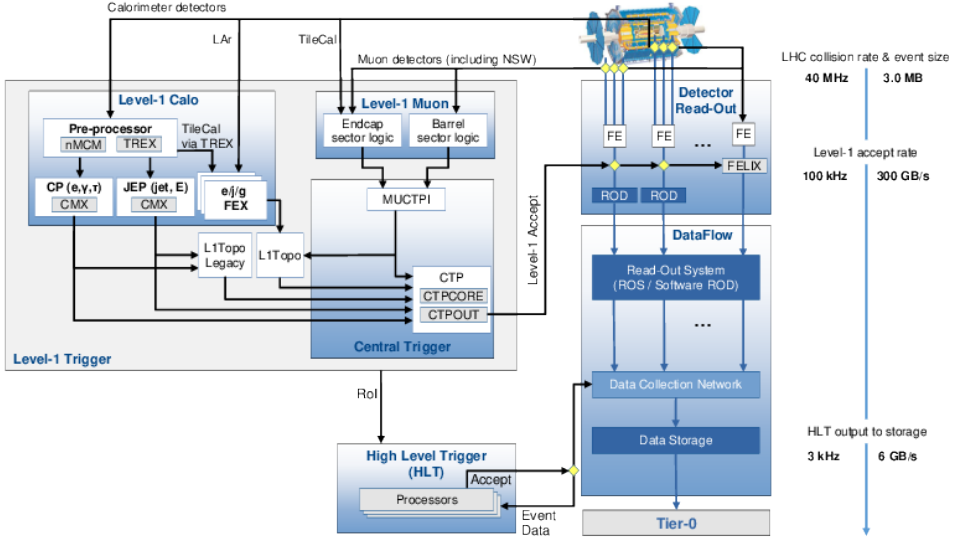


Figure 1: The ATLAS trigger system configuration for Run 3. More detailed information about the trigger configuration is available from the source of this diagram in Ref. [1]. The arrows in the diagram indicate the flow of information through the trigger system and the input rates to each level and the data throughput or bandwidth is shown on the right-hand side of the diagram.

selections on coarsely (in  $\eta$ ,  $\phi$ , and  $p_T$  or  $E_T$ ) reconstructed objects, which identifies regions of interest (RoIs) flagged for further selections. The detector readout systems limit the peak output rate of the L1 trigger to 100 kHz [1]. The L1 RoIs are transmitted to the High-Level Trigger (HLT) comprised of a CPU farm that runs more advanced algorithms similar to those used for offline reconstruction. The HLT selection determines which data is stored on disk and reconstructed offline for analysis, providing a data rate up to 3 kHz.

During 2022, jets were first reconstructed within the Run 2 Legacy L1 system using a sliding window algorithm [2]. Improvements, including better pile-up<sup>2</sup> rejection and jet reconstruction, to the L1 jet trigger from the jFEX and gFEX upgraded L1 boards will be exploited once they are fully commissioned [1]. In the Run 3 HLT jet trigger anti- $k_t$   $R = 0.4$  (small- $R$ ) jets are built from either calorimeter clusters (topoclusters, three-dimensional clusters of calorimeter cells [3]) or Particle Flow objects [4] (combining topoclusters with charged particle tracks from the inner detector) depending on the trigger algorithm requirements. These jets are reconstructed from the complete detector readout (full-scan) and are not limited to region of interest reconstruction. The extensive use of charged particle tracking within the jet trigger during Run 3 will improve the spatial and

<sup>2</sup>Additional (simultaneous) interactions in a proton-proton bunch-crossing aside from the interaction one is interested in.

momentum resolution of trigger-level (HLT) jets compared to calorimeter jets as shown for offline<sup>3</sup> jets in [4], and allows for improved pile-up rejection.

The CPU cost of full-scan charged particle tracking is significant, and increases as the LHC collision pile-up levels increase. Consequently, several CPU cost reduction strategies have been implemented, including:

**Calorimeter jet pre-selections** Trigger chains (a chain of L1 and HLT selections) running Particle Flow reconstruction at the HLT include an intermediate step where a selection is first applied to calorimeter jets. This *pre-selection* reduces the number of events for which full-scan tracking must be performed at the HLT and therefore the CPU cost of the trigger.

**Fast  $b$ -jet identification ( $b$ -tagging)** For trigger signatures selecting events with  $b$ -jets (jets originating from  $b$  quarks) where a calorimeter jet pre-selection is not suitable, fast machine learning  $b$ -tagging algorithms are applied to calorimeter jets reducing the trigger rates before more precise  $b$ -tagging is performed. This is referred to as the fast  $b$ -tagging pre-selection and discussed more in Ref. [5] with further performance results provided in [6]. In Run 3, where  $HH \rightarrow b\bar{b}b\bar{b}$  events are selected with a high-rate L1 trigger (8 kHz), the fast  $b$ -tagging pre-selection provides between a factor of 5 or 10 rejection of L1 triggered events with only a 2% or 4% loss of the  $HH \rightarrow b\bar{b}b\bar{b}$  event acceptance [5].

HLT jets are calibrated using a sequential calibration sequence similar to that applied to offline jets, derived using Monte Carlo simulation for all steps aside from the final *in situ* correction [7, 8]. The full calibration sequence applied to offline anti- $k_t$   $R = 0.4$  jets is summarised in Figure 2. The sequence begins with two corrections applied to remove pile-up radiation from jets before a scaling of the jet 4-momentum to reproduce the energy scale of simulated jets. The final stages of the calibration sequence consist of corrections for the flavour (quark or gluon) dependence of jet features and a final *in situ* 4-momentum scaling correcting the jet energy scale to that observed in data. More detail on the calibration of jets is available in Ref. [7, 8].

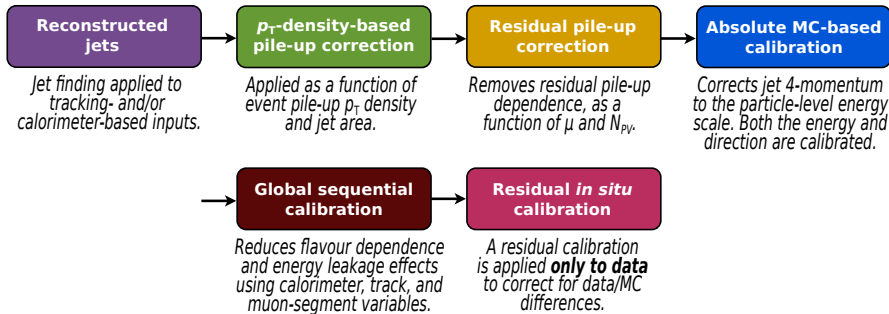


Figure 2: The calibration sequence for offline anti- $k_t$   $R = 0.4$  jets. An identical calibration sequence is applied to HLT jets. Diagram from Ref. [7].

## 1.2 Trigger-Level Analysis within the jet trigger

The physics objects, including jets, reconstructed in the HLT can be used directly (i.e. without a second more precise reconstruction of *offline* jets using raw detector data) for new physics

<sup>3</sup>Jets reconstructed from full raw detector information stored offline.

searches exploiting non-standard data-taking strategies. The selection of data for analysis using offline information is limited by the trigger bandwidth defined:

$$\text{bandwidth} = \text{trigger rate} \times \text{event size}. \quad (1)$$

The trigger rate is measured in Hz and the event size is measured in MB providing the bandwidth in units of MB/s, representative of the amount of data that is stored per second. When offline objects are analysed, the complete raw detector readout is stored, producing large event sizes on the order of 1.5 MB in Run 3. Consequently, it is necessary to apply stringent trigger selections that drastically reduce trigger rates to avoid exceeding bandwidth limitations imposed by the infrastructure used to transfer data from the HLT CPU farm to storage. Bandwidth savings by means of this trigger rate reduction reduce the acceptance of events containing low- $p_T$  jets (or other physics objects). As shown in Figure 3 this limits the kinematic range accessible with dijet resonance searches targeting low-mass dark matter mediators. The blue line for offline jets in Figure 3 has a plateau at low- $m_{jj}$  where the single jet triggers are *prescaled* meaning that events passing the trigger selection are thrown away to control the rate at which it fires. The red line for offline jets corresponds to the distribution after prescale corrections where events are weighted appropriately to recover the expected event yield in each bin. An alternative data-taking strategy called *Trigger-Level Analysis* (TLA) (discussed in detail in Ref. [9]) consists of storing only the physics objects<sup>4</sup> reconstructed in the HLT to a dedicated event stream, reducing the event size to  $\sim 5$  kB in 2022. This allows higher rate triggers (with looser kinematic selections) to be used for data collection, recovering the acceptance of low-mass and low- $p_T$  signatures lost with standard strategies (black points in Figure 3). This permitted constraints to be set on dark matter mediators with masses as low as 450 GeV in an early Run 2 TLA search [10]. Similar techniques are used by CMS (Data Scouting) [11] and LHCb (Turbo Stream) [12].

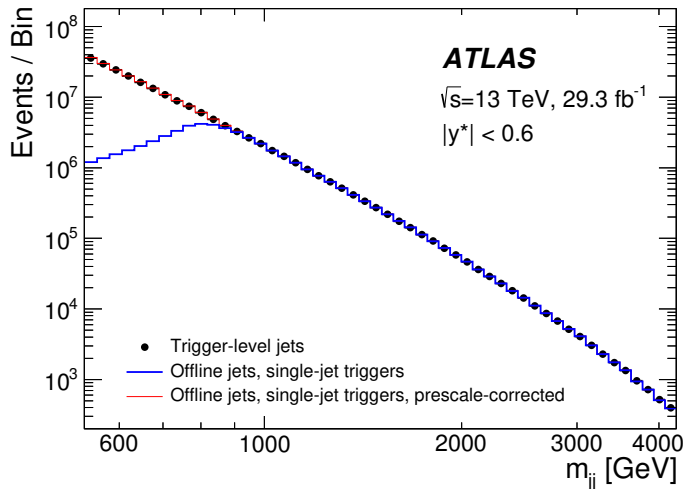


Figure 3: A Run 2 data dijet invariant mass ( $m_{jj}$ ) spectrum for offline jets in events collected with single jet triggers (blue and red lines) and HLT jets (black points; *Trigger-Level Analysis*). Plot from Ref. [10].

<sup>4</sup>For Run 3 this includes jets (Particle Flow and calorimeter only) and photons with the additional capability to store muons. By contrast, during Run 2 only calorimeter jets were stored in the Trigger-Level Analysis stream.

Since Trigger-Level Analyses rely solely on the physics objects reconstructed in the HLT it is important that each object is both well-reconstructed and well-calibrated. For the case of jet-based Trigger-Level Analyses, good calibration performance ensures the accuracy of search results, but also improves the ATLAS-wide physics performance for any signatures reliant on jet triggers.

## 2 Performance of single-jet triggers and the High-Level Trigger jet calibration

### 2.1 Single-jet trigger performance in 2022 data-taking

The performance of various single jet trigger selections in the full 2022 proton-proton collision dataset<sup>5</sup> is summarised by the trigger efficiency turn-on curves for a complete HLT and L1 trigger selection in Figure 4. The trigger efficiencies are shown as a function of the leading offline Particle Flow jet  $p_T$ . In Figure 4 both the offline and HLT jets must be reconstructed within  $|\eta| < 2.8$ . The HLT jets are corrected using a calibration configured for Run 2 reconstruction, which was used during 2022 data-taking. By contrast, the offline jets are corrected with a calibration configured for Run 3 reconstruction, which was derived after Run 3 data-taking began. The trigger efficiencies are calculated using a bootstrap method where a more inclusive trigger selection defines an unbiased reference sample from which the efficiency of the probe trigger with a higher HLT jet  $p_T$  threshold can be determined. Sharp efficiency turn-ons (a transition from low to high efficiency) indicate good trigger performance, which is commonly a result of close agreement between the energy scales of HLT and offline jets. The 99% efficiency points for the triggers shown in Figure 4 in ascending order by trigger threshold are: 41 GeV, 55 GeV, 131 GeV, 185 GeV, 271 GeV, 376 GeV, and 441 GeV. Mismatches between the reconstruction software configuration and the pile-up conditions of Monte Carlo samples used to derive the HLT and offline jet calibrations impact the sharpness of trigger efficiency turn-ons and plateau locations derived from 2022 data. As shown in Section 2.2, this mismatch results in the HLT jets having on average 5-7% higher  $p_T$  than a matched offline jet (with  $p_T$  between 25 GeV and 200 GeV) for the 2022 HLT jet calibration shown. Accordingly, the trigger efficiency plateaus would be shifted to lower  $p_T$  than for the case where the HLT jet  $p_T$  agrees more closely with the  $p_T$  of the matched offline jet. The HLT jet calibration was updated in 2023 to correct these calibration differences and further studies using 2023 data are required to quantify the trigger efficiency improvement provided by the updated calibration.

### 2.2 High-Level Trigger jet calibration performance

The agreement of HLT and offline jet energy scales has implications both for trigger efficiencies and for the calibration strategy used in Trigger-Level Analyses where the energy scale of HLT jets is corrected to that of offline jets [10]. To measure the HLT jet calibration performance with respect to offline jets we calculate the HLT/Offline jet  $p_T$  response in dijet Monte Carlo samples using fully calibrated simulated jets. The jet  $p_T$  response is constructed as the ratio of the HLT jet  $p_T$  to that of  $\Delta R < 0.3$  matched offline jets. For performant HLT jet calibrations, the response should be peaked close to 1 with a narrow width as shown in Figure 5. The response distributions are fit with Gaussians to extract the mean response, and the 68% quantiles of the response distribution are used as a measure of the width due to the presence of non-Gaussian tails in low- $p_T$  bins from detector effects such as pile-up radiation contamination.

---

<sup>5</sup>With quality requirements applied to remove runs or periods during runs where detector issues were encountered.

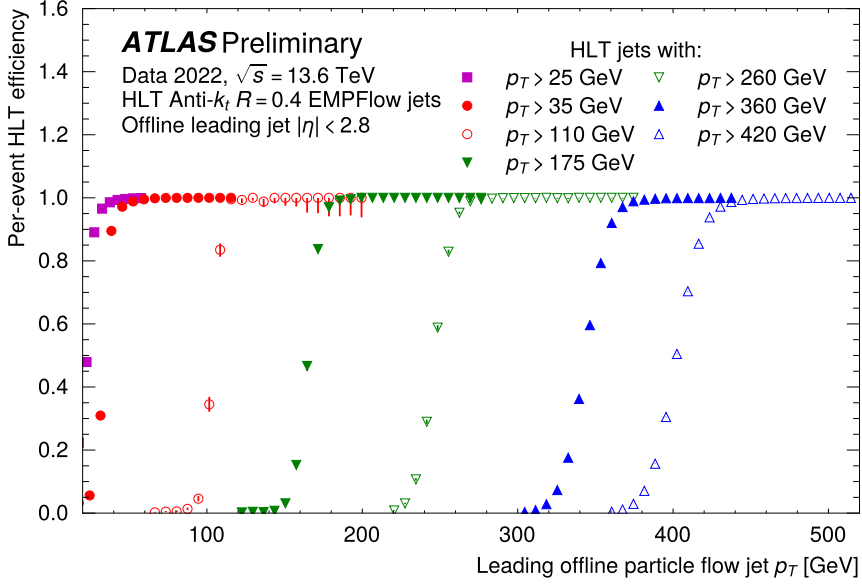


Figure 4: Trigger efficiency for single jet HLT selections as a function of the offline Particle Flow jet  $p_T$ . Plot from Ref. [13].

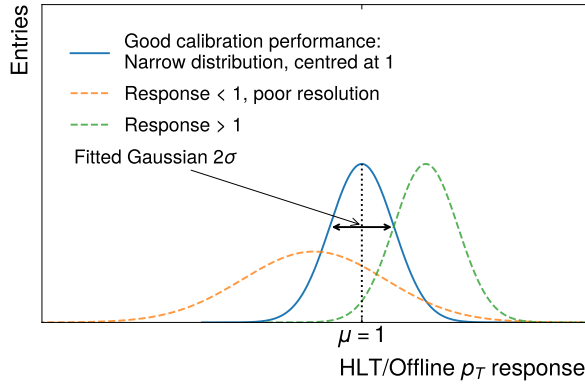


Figure 5: Illustration of the HLT/Offline jet  $p_T$  response for different cases of calibration performance.

In Figure 6 the fitted (Gaussian mean) HLT/Offline jet  $p_T$  response is shown with points surrounded by dashed lines indicating the 68% quantile boundaries for the two-dimensional response histogram (response versus  $p_T$  as in the background of Figure 6b). For consistency with collision data plots, three random L1 seeded<sup>6</sup> single jet triggers are used to cover the  $p_T$  range from 25 GeV to 200 GeV requiring  $p_T$  greater than 15 GeV, 25 GeV, and 35 GeV

<sup>6</sup>A randomly chosen L1 trigger selects events before a single jet selection is applied in the HLT.

respectively. Additionally, out-of-time pile-up jets are rejected by requiring the absolute value of the offline jet timing to be  $\leq 12.5$  ns.

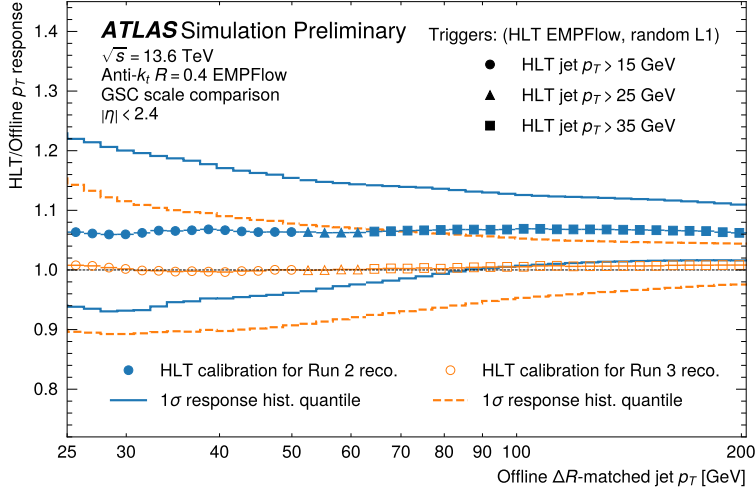
In Figure 6a (blue solid points) the HLT/Offline jet  $p_T$  response is offset by 5-7% above unity when the HLT jets calibration used for 2022 data-taking is compared to offline jets corrected with a calibration configured for Run 3 reconstruction<sup>7</sup>. The offset is a consequence of both the mismatching reconstruction configurations and differences between the Monte Carlo sample conditions (e.g. pile-up levels) used to derive each calibration introduced in Section 2.1. Applying the offline jet calibration configured for Run 3 reconstruction to the HLT jets (orange empty points in Figure 6a) reduces the offset of the jet  $p_T$  response and the surrounding 68% quantile boundaries are on average  $\sim 15\%$  narrower than for the 2022 configuration. The improved two-dimensional response histogram is shown individually in Figure 6b, and the 2022 HLT jet calibration has been replaced by the newer offline jet calibration configured for Run 3 reconstruction during 2023 data-taking.

### 3 Summary

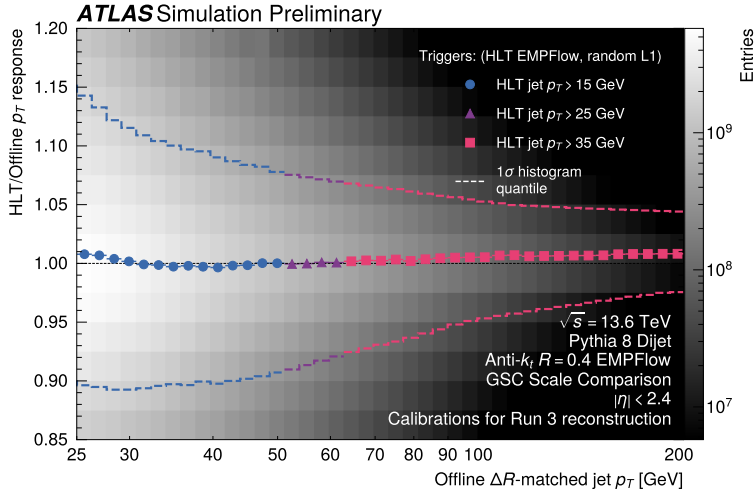
The ATLAS jet trigger for Run 3 incorporates several new features including Particle Flow jet reconstruction and multiple CPU cost mitigation strategies to support data-taking in the increasingly demanding LHC proton-proton collision conditions. Sharp trigger efficiency turn-ons are seen for various single jet High-Level Trigger selections in 2022 data. Improvements to these trigger efficiencies are expected for 2023 data-taking where mismatches between trigger-level and offline jets are resolved by applying an updated calibration to HLT jets. In the future, better HLT-offline jet agreement resulting from the use of a dedicated HLT jet calibration is expected to improve the performance of a range of jet-based trigger signatures both for Trigger-Level Analyses and standard data-taking strategies. Additionally, the commissioning of upgraded L1 trigger boards (jFEX and gFEX) for physics data-taking will improve the performance of trigger-level jet reconstruction even before events reach the HLT, having positive flow-on effects for HLT jet trigger performance.

---

<sup>7</sup>The distinction between Run 2 and Run 3 reconstruction configurations results from significant updates to the reconstruction software.



(a) HLT/Offline jet  $p_T$  response expected performance comparison of corrections for 2022 (calibration configured for Run 2 reco.) and 2023 (calibration configured for Run 3 reco.) data-taking.



(b) HLT/Offline jet  $p_T$  response expected for 2023 data-taking.

Figure 6: The HLT/Offline jet  $p_T$  response in dijet Monte Carlo simulation for fully calibrated simulated jets as a function of the matched offline Particle Flow jet  $p_T$ . Plots from Ref. [13].



## References

- [1] The ATLAS Collaboration, Tech. rep., CERN, Geneva (2023), 2305.16623, <https://cds.cern.ch/record/2859916>
- [2] R. Achenbach, P. Adragna, V. Andrei, P. Apostologlou, B. Åsman, C. Ay, B.M. Barnett, B. Bauss, M. Bendel, C. Boehm et al., *Journal of Instrumentation* **3**, P03001 (2008)
- [3] The ATLAS Collaboration, *Eur. Phys. J. C* **77**, 490 (2017), 1603.02934
- [4] The ATLAS Collaboration, *Eur. Phys. J. C* **77**, 466 (2017), 1703.10485
- [5] The ATLAS Collaboration, Tech. rep. (2023), 2306.09738, <https://cds.cern.ch/record/2862499>
- [6] The ATLAS Collaboration, *Public b-Jet Trigger Plots for Collision Data* (2023), <https://twiki.cern.ch/twiki/bin/view/AtlasPublic/BJetTriggerPublicResults>
- [7] The ATLAS Collaboration, *Eur. Phys. J. C* **81**, 689 (2021), 2007.02645
- [8] The ATLAS Collaboration (ATLAS), Tech. rep., CERN, Geneva (2023), 2303.17312, <https://cds.cern.ch/record/2854733>
- [9] The ATLAS Collaboration, Tech. rep., CERN, Geneva (2017), <https://cds.cern.ch/record/2295739>
- [10] The ATLAS Collaboration, *Phys. Rev. Lett.* **121**, 081801 (2018)
- [11] S. Mukherjee, *PoS EPS-HEP2019*, 139 (2020)
- [12] S. Benson, V. Gligorov, M.A. Vesterinen, J.M. Williams, *Journal of Physics: Conference Series* **664**, 082004 (2015)
- [13] The ATLAS Collaboration, *Public Jet Trigger Plots for Collision Data* (2023), <https://twiki.cern.ch/twiki/bin/view/AtlasPublic/JetTriggerPublicResults>